AlGaN/GaN double-channel HEMT

Quan Si(全思)†, Hao Yue(郝跃), Ma Xiaohua(马晓华), Zheng Pengtian(郑鹏天), and Xie Yuanbin(谢元斌)

(Xidian University, Xi'an 710126, China)

Abstract: The fabrication of AlGaN/GaN double-channel high electron mobility transistors on sapphire substrates is reported. Two carrier channels are formed in an AlGaN/GaN/AlGaN/GaN multilayer structure. The DC performance of the resulting double-channel HEMT shows a wider high transconductance region compared with single-channel HEMT. Simulations provide an explanation for the influence of the double-channel on the high transconductance region. The buffer trap is suggested to be related to the wide region of high transconductance. The RF characteristics are also studied.

Key words: high-electron mobility transistor; AlGaN/GaN/AlGaN/GaN; double-channel
DOI: 10.1088/1674-4926/31/4/044003 **EEACC:** 2520

1. Introduction

The AlGaN/GaN high electron mobility transistor (HEMT) is an excellent candidate for applications in high power electronics. Superior performance of the AlGaN/GaN HEMT relies on the high breakdown electric field of nitride semiconductors and the polarization effect-induced high-density high-mobility two-dimensional electron gas (2DEG) at the AlGaN/GaN interface[1−3]. AlGaN/GaN double-channel HEMTs were constructed to enhance the current drive[4] and to alleviate the current collapse[5]. In this paper, we report a double-channel HEMT with low electron density in the second channel. Wider high transconductance region is obtained compared with single-channel HEMT. The simulation results dictate that buffer trap is a leading factor to diminish the high transconductance region in a single-channel device, while in a double-channel device, the high transconductance region is not affected by the buffer trap.

2. Device structure and fabrication

The AlGaN/GaN/AlGaN/GaN HEMT layers were grown by metal organic chemical vapour deposition (MOCVD) on (0001) sapphire substrate. As depicted in Fig. 1, the layered structure consists of a 1.2-μm-thick undoped GaN buffer layer, a 8-nm-thick AlGaN bottom barrier layer with Al composition of 8%, a 20-nm-thick GaN channel layer, and a 20-nm-thick $Al_{0.3}Ga_{0.7}N$ top barrier layer.

The measured Hall mobility and sheet electron density are 1030 $cm^2/(V{\cdot}s)$ and 1.6×10^{13} cm^{-2} at room temperature. C–V measurements were carried out to profile the carrier distribution, showing that there are two electron channels with a 30-nm peak-to-peak separation (Fig. 2). The two electron channels are located at the upper and lower AlGaN/GaN interfaces of the AlGaN/GaN/AlGaN/GaN multilayer structure respectively, with the electron density of the bottom electron channel much less than that of the upper one. The low electron density in the bottom channel is attributed to the thin layer and low Al composition of the AlGaN bottom barrier layer.

The devices were fabricated on the AlGaN/GaN/AlGaN/GaN epilayer described above. Mesa isolation was formed by ICP with the etch-depth of 200 nm. Ohmic contacts consisting of Ti/Al/Ni/Au (22 nm/140 nm/55 nm/45 nm) were annealed in a nitrogen ambient at 850 °C, yielding a contact resistance typically around 1.0 Ω·mm. Passivation film Si_3N_4 was deposited on the sample by PECVD. Then the gate windows with 0.7 μm

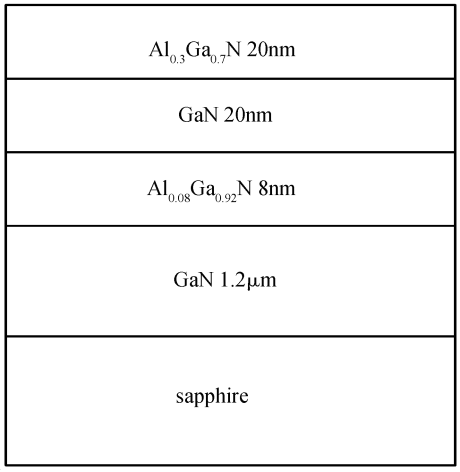

Fig. 1. Cross-sectional schematic of an AlGaN/GaN/AlGaN/GaN epilayer on sapphire substrate.

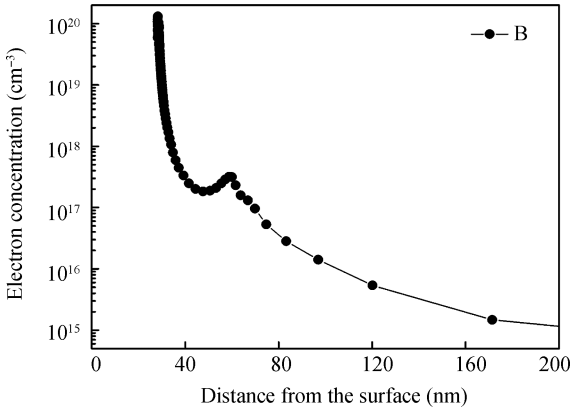

Fig. 2. Electron distribution profile of AlGaN/GaN/AlGaN/GaN epilayer.

† Corresponding author. Email: siquan@163.com
Received 9 December 2009

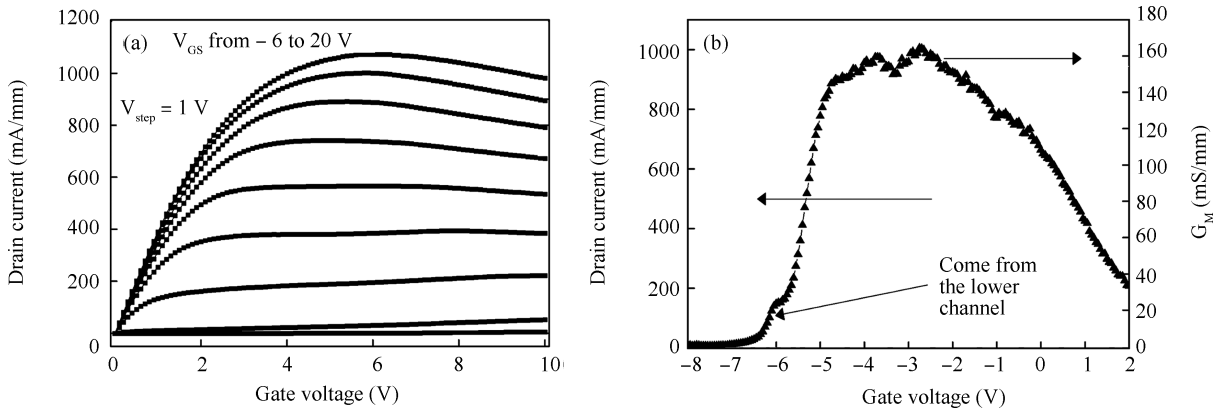

Fig. 3. (a) DC I–V output and (b) transfer characteristics of a double-channel device.

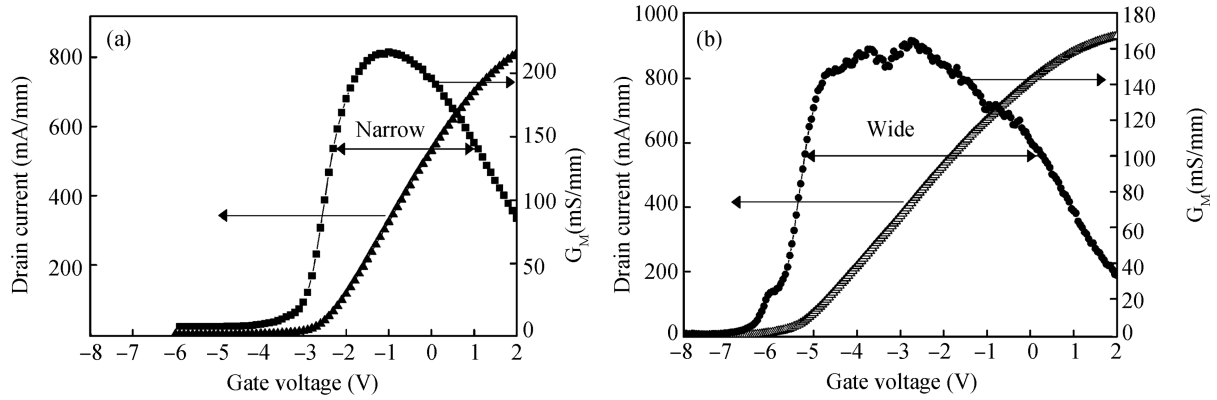

Fig. 4. Transfer characteristics of (a) a single-channel device and (b) a double-channel device.

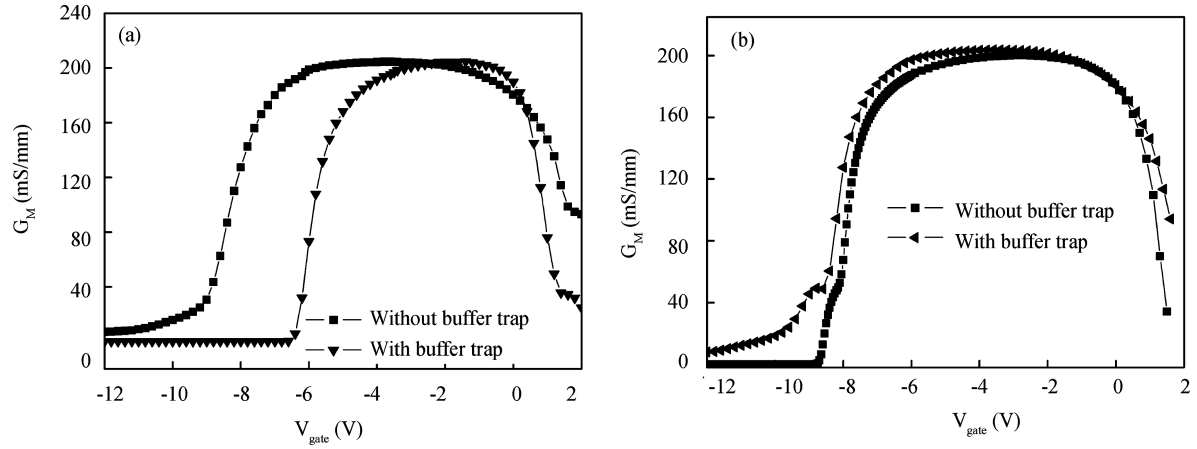

Fig. 5. Simulated transconductance g_m versus V_{GS} at V_{DS} = 10 V for (a) single-channel device with and without buffer trap and (b) double-channel device with and without buffer trap.

gate length were opened by photolithography, followed by CF_4 plasma treatment in a reactive ion etching (RIE) system. Finally, the Ni/Au Schottky gate was deposited by electron-beam evaporation. Direct current characteristics and high frequency characteristics were measured by Agilent 1500B semiconductor parameter analyzer and Agilent E8363B network analyzer.

3. Results and discussion

The DC output and transfer characteristics of 100-μm-wide device are plotted in Figs. 3(a) and 3(b). The device exhibits a peak current density of 1.07 A/mm and a peak transconductance of 164 mS/mm. From Fig. 3(b), we can observe a double-hump structure in the G_M versus gate bias (V_{GS}) curve, which corresponds to the effective gate modulation of the upper and the lower 2DEG channel respectively. The secondary hump is small because the 2DEG density is low in the bottom channel. Figures 4(a) and (b) show the comparison of transfer characteristics between single-channel device and double-channel device. The two devices are fabricated in the same process. The high transconductance region of the double-channel device is wider than that of the single-channel device, with the $G_{M,max}$

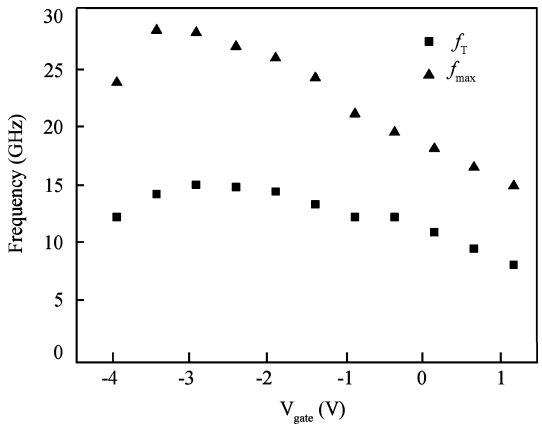

Fig. 6. Dependence of f_T and f_{max} on gate bias.

lower than that of single-channel device.

In order to understand the mechanism of the wide high transconductance region, simulation is taken into study. As shown in Fig. 5, buffer trap is a leading factor to minish the high transconductance region in single-channel device, and in double-channel device, small transconductance hump is minished by the buffer trap while the large transconductance hump is not affected by the buffer trap. In double-channel device, the 2DEG in the lower channel would be trapped by the buffer trap, while the 2DEG in the upper channel would not be trapped by the buffer trap because there is a barrier between the upper channel and the buffer.

RF small-signal characterization was performed on the double-channel device by measuring S-parameters at a variety of gate bias points (Fig. 6). At the optimum bias point, extrinsic cutoff frequency (f_T) and maximum oscillation frequency (f_{max}) of double-channel device are 15 GHz and 28 GHz, respectively. From Fig. 6, we can see a wide operation range of double-channel device.

4. Summary

An AlGaN/GaN/AlGaN/GaN double-channel high electron mobility transistor on sapphire substrate has been demonstrated. Device with double channel shows a wide high transconductance region compared with device with single channel. Simulations show that in single-channel device, high transconductance region is diminished by buffer trap, while in the double-channel device, the primary channel is free from the buffer trap, thus the high transconductance region is not affected by the buffer trap.

References

[1] Ambacher O, Smart J, Ahealy J R, et al. Two-dimensional electron gases induced by spontaneous and piezoelectric polarization charges in N- and Ga-face AlGaN/GaN heterostructures. J Appl Phys, 1999, 85: 3222

[2] Yu E T, Dang X Z, Asbeck P M, et al. Spontaneous and piezoelectric polarization effects in III–V nitride heterostructures. J Vac Sci Technol B: Microelectron Process Phenom, 1999, 17: 1742

[31] Ibbetson J P, Fini P T, Ness K D, et al. Polarization effects, surface states, and the source of electrons in AlGaN/GaN heterostructure field effect transistors. Appl Phys Lett, 2000, 77: 250

[4] Gaska R, Shur M S, Fjeldly T A, et al. Two-channel AlGaN/GaN heterostructure field effect transistor for high power applications. J Appl Phys, 1999, 85: 3009

[5] Chu R, Zhou Y, Liu J, et al. AlGaN-GaN double-channel HEMTs. IEEE Trans Electron Devices, 2005, 52: 438